IRAQI Academic Scientific Journals

Tikrit Journal of Engineering Sciences (2020) 27 (3): 82-93

ISSN: 1813-162X (Print) ; 2312-7589 (Online)

Tikrit Journal of Engineering Sciences

available online at: http://www.tj-es.com

College of Engineering

TJES Tikrit Journal of Engineering Sciences

Raed N. Razooqi, **Omar J. Abdulkareem**. **Influences of Mg Addition on the Mechanical Properties of Cu-Al-Ni Shape Memory Alloys**. *Tikrit Journal of Engineering Sciences* 2020; **27**(3): 82- 93.

Raed N. Razooqi

Omar J. Abdulkareem*

Department of Mechanical Engineering / Collage of Engineering / Tikrit University / Tikrit, Iraq

Influences of Mg Addition on the Mechanical Properties of Cu-Al-Ni Shape Memory Alloys

***Keywords*:**

Shape memory alloys, SMAs, Magnesium, Cu-Al-Ni, Mechanical properties, Copper based.

A R T I C L E I N F O

Article history:

Received	11 Sep. 2018
Accepted	31 Dec. 2018
Available online	01 July 2020

A B S T R A C T

Shape Memory Alloys (SMAs) are a unique class of material that possesses unconventional properties such as the shape's memory effect, the high flexibility associated with damping capabilities, high wear resistance and fatigue. Given its use in a variety of technological applications, its studies have attracted increased interest in the community of scientists and researchers during the past decades.

The shape memory alloy (Cu 83%-Al 13%-Ni 4%) and the other alloy with adding the alloying elements (Mg) with content of (0.25, 0.5, 0.75, 1.0, 1.25) % as a volumetric ratio which was taken from the copper percentage were prepared by powder metallurgy, The powders were mixed using (V-type) powders mixer with mixing speed and time (20 rpm), (16 min) respectively then the samples were pressed by a two-way press (floating die) and pressing pressure (500 MPa) then the green samples where sintered by using vacuum furnace with using Argon gas medium at a temperature (900°C) for one hour and left in the oven to cool down to room temperature.

The results showed that both bulk density and apparent density compared to the base alloy increase by increasing the volumetric fraction of Mg by the ratios (5.49)% compared to the bulk density of the base alloy and by the ratios (1.51)% compared to the apparent density of the base alloy. accompanied by a decrease in the real and apparent porosity and water absorption, The results of the mechanical tests showed an increase in the hardness and diametrical compressive strength with the increase of volumetric fraction of (Mg) compared to the base alloy accompanied by a decrease in the rate of wear, The (XRD) test observes the composing phases (α(Cu4Al), β(Cu3Al), γ(Cu9Al44)) in addition to determining the transformation temperature from the Martensite to the Austenite by examining the (DSC) it was found that the Austenite initiation and finish (As), (Af) increased by adding the alloying elements (Mg).

DOI: http://doi.org/10.25130/tjes.27.3.10

* *Corresponding author: E-mail:* omaralkaylany@tu.edu.iq

تأثير اضافة المغنيسيوم على الخصائص الميكانيكية للسبيكة الذاكرة للشكل(Cu-Al-Ni) المحضرة بتقانة تكنولوجيا المساحيق

عمر جمال عبد الكريم قسم الهندسة الميكانيكية ، كلية الهندسة ، جامعة تكريت
رائد نجيب رزوقي قسم الهندسة الميكانيكية ، كلية الهندسة ، جامعة تكريت

الخلاصة

تمثل السبائك الذاكرة للشكل (Shape Memory Alloys (SMAs فئة فريدة من المواد التي تمتلك خصائص غير تقليدية مثل التأثير الذاكر للشكل، المرونة الفائقة المرتبطة بقدرات التخميد ومقاومة التآكل والكلال العاليتين. وبالنظر لاستخدامها في مجموعة متنوعة من التطبيقات التكنولوجية، فقد لفتت دراساتها الاهتمام المتزايد في مجتمع العلماء والباحثين خلال العقود السابقة. وتم تحضير السبائك بتقانة ميتالورجيا المساحيق وبنسب (Cu -%13 Al -%4 Ni 83%) للسبيكة الاساس وقد تم اضافة العنصر Mg بالنسب % (1.25, 1.0, 0.75, 0.5, 0.25) ، تم خلط المساحيق باستخدام جهاز خلط المساحيق نوع (V) بسرعة وزمن خلط (20 min 16) ،(r.p.m) على التوالي وكبست العينات بوساطة قالب كبس (عائم) باتجاهين وبضغط كبس (500 MPa)، تم تلبيد العينات الخضراء باستخدام فرن كهربائي مفرغ من الهواء وبوسط من غاز الارغون بدرجة حرارة (900C°) لمدة ساعة واحدة وتركت العينات بالفرن لتبرد الى درجة حرارة الغرفة. وأظهرت النتائج زيادة كل من الكثافة الحجمية والكثافة الظاهرية بزيادة الكسر الحجمي للمغنيسيوم بالنسبة (5.49)% عند محتوى (1.25)% مقارنة بالكثافة الحجمية للسبيكة الاساس و بالنسبة (1.51)% عند النسبة ذاتها مقارنة بالكثافة الظاهرية للسبيكة الاساس رافقهما انخفاض في المسامية الحقيقية والظاهرية وقابلية امتصاص الماء، كما أظهرت نتائج الفحوصات الميكانيكية زيادة في الصلادة ومقاومة الانضغاطية القطرية مع زيادة الكسر الحجمي للعنصر (Mg) مقارنة بالسبيكة الاساس، توافق ذلك مع انخفاض في معدل البلى. ومن خلال فحص حيود الاشعة السينية تم التعرف على الاطوار المتكونة وهي (Cu_9Al_{44})γ ،(Cu_3Al)β ،(Cu_4Al)α)) علاوة على تحديد درجات حرارة التحول من المارتنسايت الى الاوستنايت من خلال فحص مسعر المسح التبياني اذ ازدادت كل من درجة حرارة بدء ونهاية تحول الاوستنايت (As) و (Af) بنسب مختلفة عند اضافة المغنيسيوم.

1. INTRODUCTION

Classical engineering materials such as metals and alloys have played an important role as structural materials for many centuries. Engineers have designed selected components and alloys by using the classical geometric approach to understand the macroscopic properties of the material and choose the appropriate element to match the desired function based on application. The demand for lighter, higher-resistance materials with characteristics designed to meet both design requirements and additional engineering functions (such as sensing, operation and electromagnetic protection) has led to the development of a new branch of materials called Active or Multifunctional Materials [1]. The discovery of the phase of martensite in steel in 1890 by Adolf Martens was a major step towards the eventual discovery of memory alloys. Probably the most widely studied phenomenon of metals during the early 1900s, the concept of thermal transformation and the interpretation of the reverse transformation of martensite was introduced in 1949 by Kurdjumov and his colleagues based on experimental observations of the thermally transformable martensite phase of Cu-Zn, Cu-Al alloys [2]. In 1951, the term “Shape Recovery” was first introduced by Chang and his colleague when they studied the Au-Cd alloy and observed the phase change phenomenon. Copper-based memory alloys have caught the attention of researchers because they are cheap, easy to manufacture and have good properties. Made of all materials, they are widely available and require conventional preparation and manufacturing tools (classic furnace and other tools). Parts can be produced in almost any shape and size, although the Cu-Al alloy has ductility, limited operability and good shape memory characteristics, but has a phase shift temperature. This defect can be easily reduced by adding a third element that gives it relatively stable phase. Most of the alloys studied were Cu-Zn-Al and Cu-Al-Ni, while some attention was devoted to the Cu-Al-Mn and Cu-Al-Be alloys. The most common uses of these alloys are in civil pipe fittings, hydraulic fittings, mechanical dampers, thermal actuators and sensor systems [3, 4]. J.W. KIM et al has studied the effects on microstructure and tensile properties of a Zirconium addition to a Cu-AI-Ni shape memory alloy and their results show that the addition of Zr to (Cu-A1-Ni) alloy was effective in reducing the initial grain size and suppressing the subsequent grain growth and the Fracture strength increases from 380 to 830 MPa also the fracture strain increases from (4 to 7.5) % by adding 0.54% wt of Zr [5]. Also, Safaa.N.Saud et al studied the Influence of Ag nanoparticles addition on the phase transformation, mechanical properties and corrosion behavior of Cu-Al-Ni shape memory alloys, they find that the fracture stress and strain significantly enhanced to 420 MPa and 2.35%, respectively by addition of Ag nanoparticles into Cu-Al-Ni SMA. However, the addition of Ag nanoparticles increased the shape recovery ratio from 50% to 80%. Also Polarization

tests showed that the corrosion potential of Cu-Al-Ni alloy becomes more positive after addition of Ag nanoparticles [6]. To enhance the mechanical properties of Cu-Al-Ni alloy Safaa N. Saud et al studies the influence by alloying additional elements. They found that a Co (1.14 wt%) alloy yield the best overall enhancement to the transformation temperatures, shape memory recovery and ductility. These enhancements were mainly due to the high existence of the γ2 phase in the microstructures of the modified alloy [7]. Abdul Raheem K. Abid Ali et al study the effect of adding Cr element with content of (0.3, 0.6, 0.9)% to (Cu-13Al-4Ni) shape memory alloys after compacting, sintering and quenching after heat treatment at (850^{o}C for 60 minute) then cooling in cold water (3-4^{o}C), The results show that the hardness increases and the porosity decreases with percent of Cr. The fracture compression stresses, have been increased by adding (0.3%-Cr) which had porosity (27%), and when the content of Cr is (0.9%) the porosity decreases to (22%) [8]. The shape memory effect and the microstructure of (Cu-13Al-4 Ni) high temperature shape memory alloys with contents of boron (0.25 wt%, 0.5 wt%, 1.0 wt%, and 2.0 wt%) were studied by Xin Zhang et al and there study show that the addition of boron enhanced the mechanical properties of the shape memory alloy, but also greatly improved the shape memory effect of the alloy. The martensite fracture changed from intergranular to transgranular fracture [9]. In addition and it also found that the highest shape memory effect was by adding 0.25 wt% boron . Raad S. Ahmed Adnan study the effect of Tin addition on mechanical properties and shape memory effect of Cu-Al-Ni, Pure Sn (99.99%) was added in three different percentages (0.3,1,3) %. The study show that Sn addition to the shape memory alloy has increased the transformation temperatures and also improves the shape memory properties and the best results examine was with (1%-Sn) alloy, the mechanical properties enhanced by adding Sn which raised the yield stress [10].

2. EXPERIMENTAL PART

2.1 Experimental Procedure

The powders were weighed and samples coded according to the volumetric ratios as in the Table 1. The powders were mixed using a V-Type mixer made by using an electronic microcontroller (Arduino Uno) and a stepper motor as shown in Fig.1.

Table 1.

Coding of samples, number and percentage of materials

Spec.		Ratio (%)			
Code	No.	Cu	Al	Ni	Mg
A	4	83	13	4	-
B	4	82.75	13	4	0.25
C	4	82.5	13	4	0.5
D	4	82.25	13	4	0.75
E	4	82	13	4	1
F	4	81.75	13	4	1.25

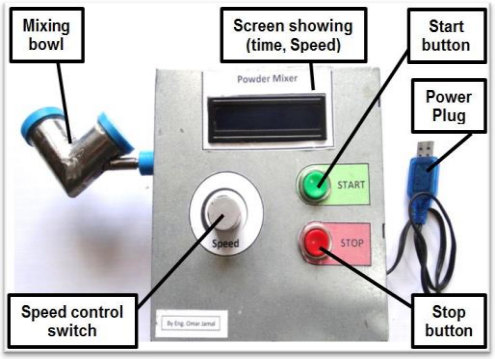

Fig.1. V-Type mixer

The mixing process in this study was done after the powders were placed in the mixing bowl according to the parameters / mixing speed (20 rpm) and time of (16 min), the powders were pressed to produce green samples using (Floating Die) as shown in the Fig.2 Then pressed with pressure (500 MPa) and retention time (60 Sec) [11], the dimensions of the green samples were (1.2mm diameter and height 5.6mm). The green specimens were placed inside electrical vacuum furnace shown in Fig.3, the internal air was discharged using a compressor (dry Pump) for about (30 min) until the absolute pressure inside the chamber was (-14 psi), the pumping of Argon gas at a pressure of (2 psi) to ensure that the air does not enter into the furnace chamber. Samples sintered at (900 ° C) according to the regime shown in Fig.4 and then slow cooling inside the oven to room temperature.

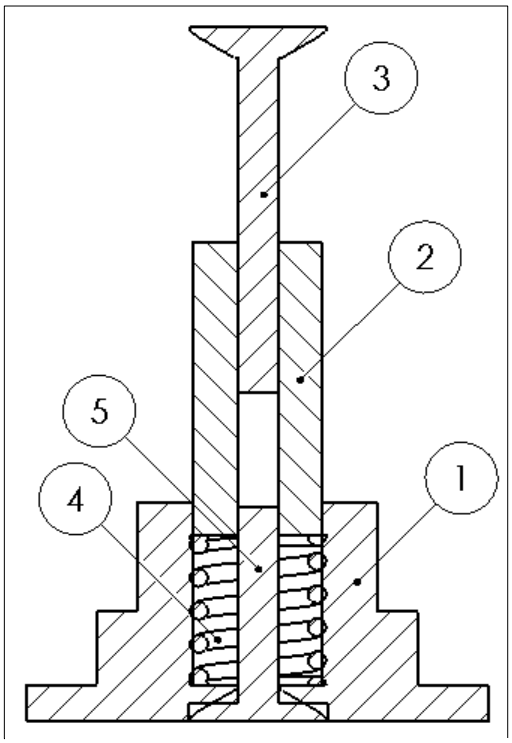

1 Die holder
2 Die
3 Upper punch
4 Spring
5 Lower Punch

Fig.2. Floating Die

Fig.3. Vacuum Furnace

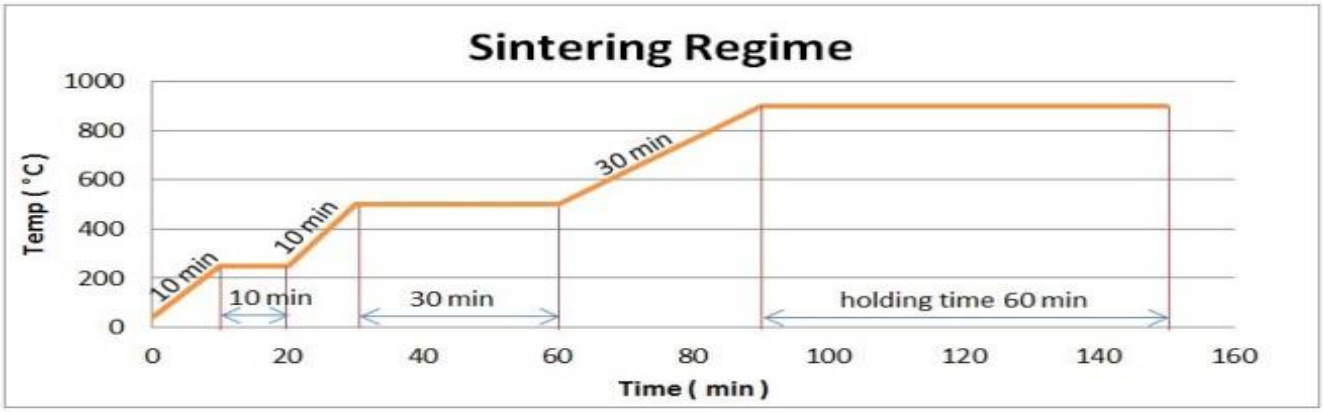

Fig.4. Sintering Regime

2.2 Physical Measurements

2.2.1 Samples Preparation

The samples were prepared for microscopic examination and hardness test by grinding and polishing the surfaces of the samples using a silicon carbide (SiC) smooth paper according to the gradient (600, 1000, 1500, 2500). The samples etched using (HCl (30 ml) + H2O (120 ml)) as etchant solution and then washed with alcohol and dried using a sample drying device (TORRAMET Specimen Dryer) to be ready for microscopic examination by optical microscope type (OLYMPUS) installed on it camera type (Amscope – FMA050 \ 9.0MP).

2.2.2 Bulk and Apparent Density, True and Apparent Porosity and Water Absorption

Bulk, apparent density, real and apparent porosity and water absorption were calculated using Archimedes' theory according to the international standard (ASTM C373-88) using a precision sensor (0.0001 g) and the following steps [12, 13]:

1. Dry weight (Wd) was calculated by weighing the samples after drying them in an electric oven at (150 ° C) for one hour.

2. The models were placed in boiling distilled water for five hours after which they were kept in distilled water at room temperature for (24 h) and then the samples were weighed after being removed from the water with the removal of the suspended surface water only and is called saturated weight (Ws).

3. Each model is weighed and suspended and immersed in water using a sensitive suspension balance. This weight is called the suspended weight (Wi).

4. The theoretical density (T.D.) was calculated using the Eq. (1) as it is defined as the ratio of mass to the actual size of the material without pores and voids.

n : Number of elements

ρi : Density (g/cm^3)

$$\text{T. D.} = \sum_{i=1}^{n} (\rho i . Xi) \quad (1)$$

Xi : Content of each element (%)

5. The Bulk Density (B.D.) and Apparent Density (A.D.), True Porosity (T.P.) and Apparent Porosity (A.P.), and Water Absorption (W.A.) were calculated using the Eq. (2 to 6).

W_d : Wight of dry specimen (g)

$$\text{A. D.} = \frac{W_d}{W_d - W_i} \times \rho_w \quad (3)$$

$$\text{A. P.} = \frac{W_s - W_d}{W_s - W_i} \times 100\% \quad (4)$$

$$\text{T. P.} = \frac{T.D. - B.D.}{T.D.} \times 100\% \quad (5)$$

$$\text{W. A.} = \frac{Ws - W_d}{W_d} \times 100\% \quad (6)$$

W_s: Wight of water saturated specimen (g)

W_i : Wight of immersed specimen (g)

ρ_w : Density of water (g/cm^3)

2.2.3 X-Ray Diffraction (XRD)

An X-ray diffraction device (SHEMADZU\ XDR-6000) was used with a copper target (CuKα1), wavelength (A 1.5405980), equipped voltage (40KV) and current (30 mA). The survey was conducted for a set of samples with a range of (10°-120°) and at a speed (5 deg/min) at room temperature. The granular size predicted from the knowledge of Full Width at Half Maximum (FWHM) [14]

2.2.4 Differential Scanning Calorimetry (DSC)

The (DSC) device (SETARAM-131 EVO) was used to determine the transformation temperatures and the completion of martensite to austenite for selected sample groups. The samples were tested by heating (C-400) at a speed of (10 C / min).

2.3 Mechanical Measurement

2.3.1 Hardness Test

Vickers hardness measuring device (MEKTON - Model \ THV-501E) was used. Five tests were conducted for each sample in different areas distributed on the surface of the sample after softening it and calculated the rate of five readings.

2.3.2 Diametrical Compressive Strength Test

A load on the sample dimensions mm (5.6 X ø11.2) until the failure occurred and installed the highest load recorded by the device through the digital screen. It should be noted here that the device has the possibility of storing the highest value of the load before the failure occurred and compression resistance was calculated from the Eq.(7)[15]:

σ_d : Diametrical Compressive Strength (MPa)
F : Applied Force (N)
h : Specimen thickness (mm)
d : Specimen diameter (mm)

$$\sigma_d = \frac{2F}{\pi d h} \quad (7)$$

2.3.3 Wear Test

The wear test was performed using Pin - On - Disk (Wear and Friction Monitor ED-201) and was tested at a speed of 740 rpm and a vertical load of (20 N) using a hardened alloy steel disc with (62 HRC) hardness, the wear rate where calculated using Eq.(8 to10) After weighing the samples before and after testing, the disc was cleaned after each test using silicon carbide paper measuring (1000) and then washing the disc with acetone [16].

$$\text{Wear Rate} = \frac{\Delta W}{S} \quad (8)$$

$$\Delta W = W_1 - W_2 \quad (9)$$

$$S = 2\pi rtn \quad (10)$$

W_1 : Wight of specimen before test (g)
W_2 : Wight of specimen after test (g)
r : Radius of sliding (cm)
t : Time of test (min)
n : Rotation speed (r.p.m)

3. RESULTS AND DISCUSSION

The experimental results reached at in this work can be categorized as follows:

3.1 Bulk and Apparent Density, True and Apparent Porosity, and Water Absorption

The addition of magnesium to the shape memory alloy of Cu-Al-Ni increased the Bulk density as shown in Fig.5 as it reached its highest value at magnesium ratio (1.25%), the increase in bulk density was (5.49%).

Although the magnesium density is lower than that of copper, the low meltingtemperature of the magnesium below the sintering temperature has led to the smelting of magnesium, thus filling the interstitial spaces and increasing the bulk density.

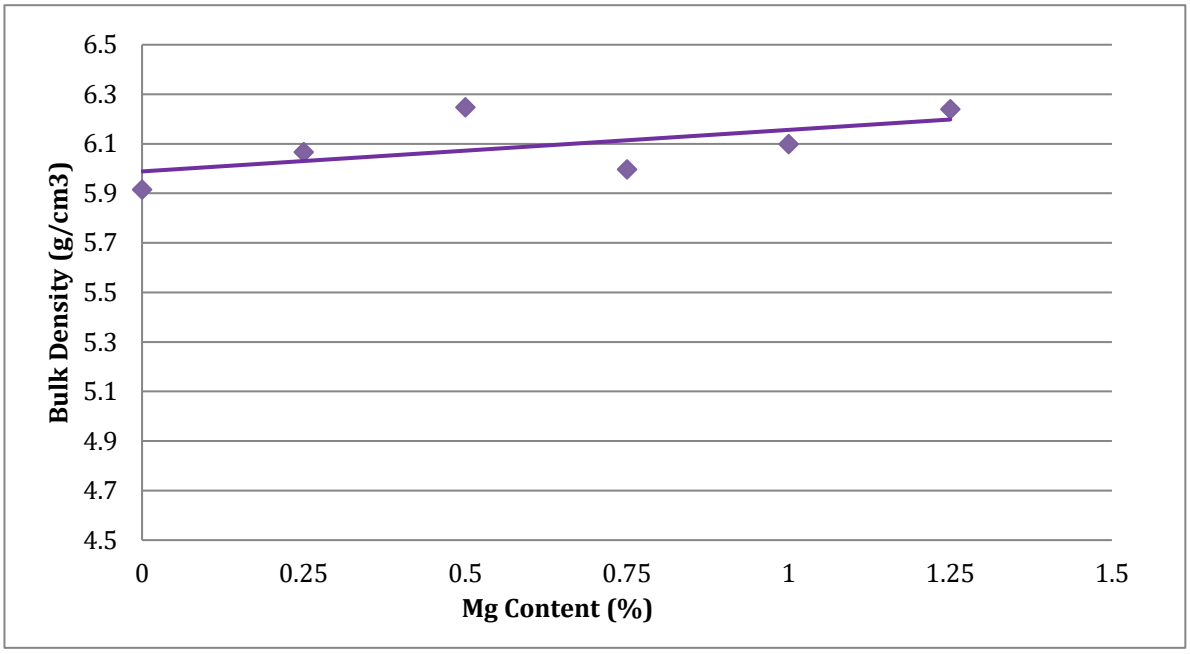

Fig.5. Influence of Mg content on Bulk Density

Also, the effect of increasing magnesium fracture on Cu-Al-Ni memory alloy has led to a slight increase in the apparent density to reach its highest value at magnesium ratio (1.25%) which is 1.51% higher than (17.69%) to the real porosity value of the base alloy, The apparent porosity decreased by increasing the volumetric fraction of magnesium to reach its lowest value at magnesium ratio (1.25%) as it decreased by

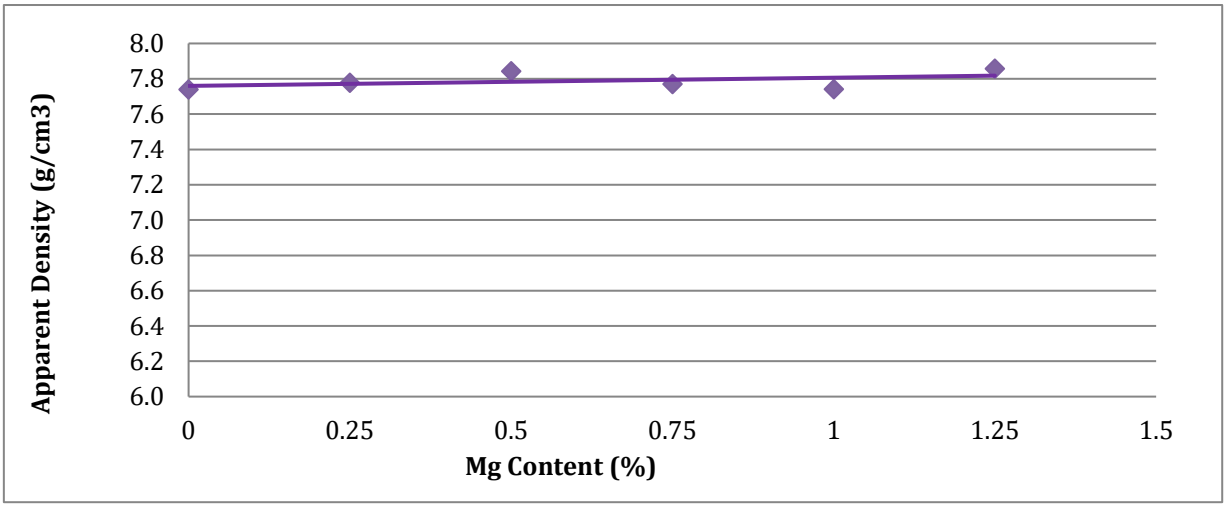

Fig.6. Influence of Mg content on apparent Density

the base alloy apparent density Fig.6. This is consistent with the behavior of the relation of the volumetric fraction of the alloy to the bulk density. The addition of magnesium decreased the true porosity to reach its lowest value at the magnesium ratio (1.25%) as it was (12.68%) to the apparent porosity value of the base alloy. In addition, the water absorption capacity of the alloy decreased by increasing the volumetric fraction of magnesium until it reached its lowest value at the ratio of magnesium (1.25%). (Open pores).

3.2 Hardness

The effect of magnesium addition on hardness of Cu-Al-Ni is shown in Fig.7, which shows the increase of hardness by increasing the magnesium fraction as it reached its highest value by (39.0%)% compared to the base alloy hardness. The reason for the increase is attributed to the observed data of (XRD) in Fig.8 and compacting and bonding of the components.

Table 2, which shows the increase in the value of (FWHM) which indicates the decrease of the granular size from the base alloy in addition to the increase in the percentage Sedimentation increases magnesium content Figs. 9 and 10, The increase in volume and apparent densities increases the hardness value as an indicator of

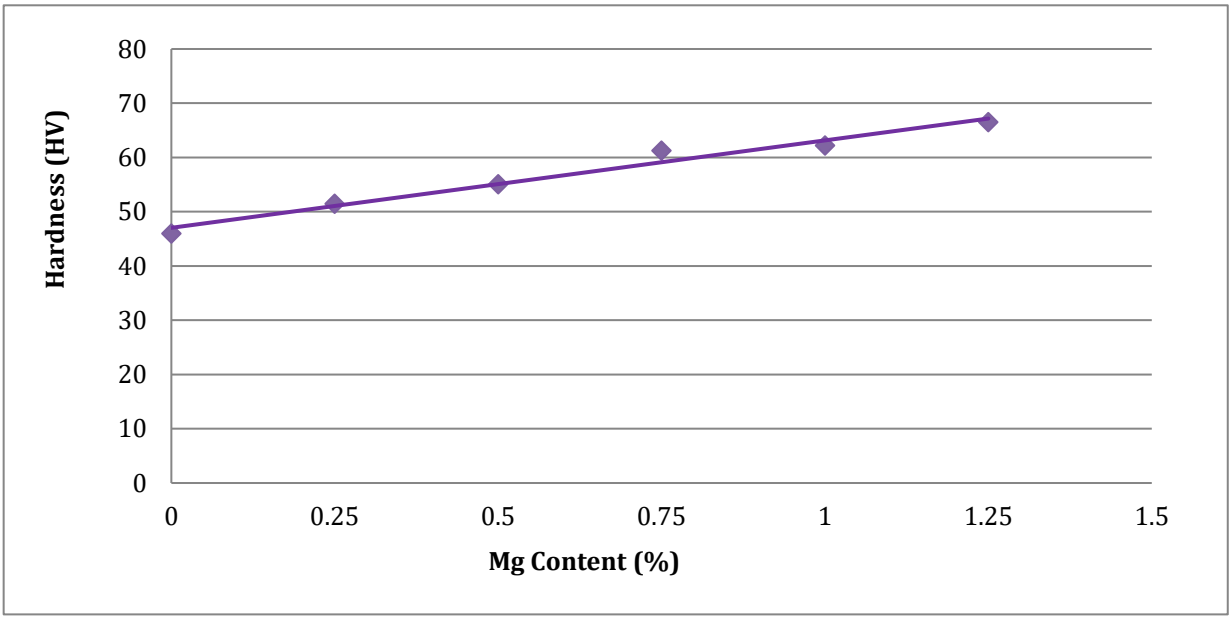

Fig.7. Influence of Mg content on Hardness

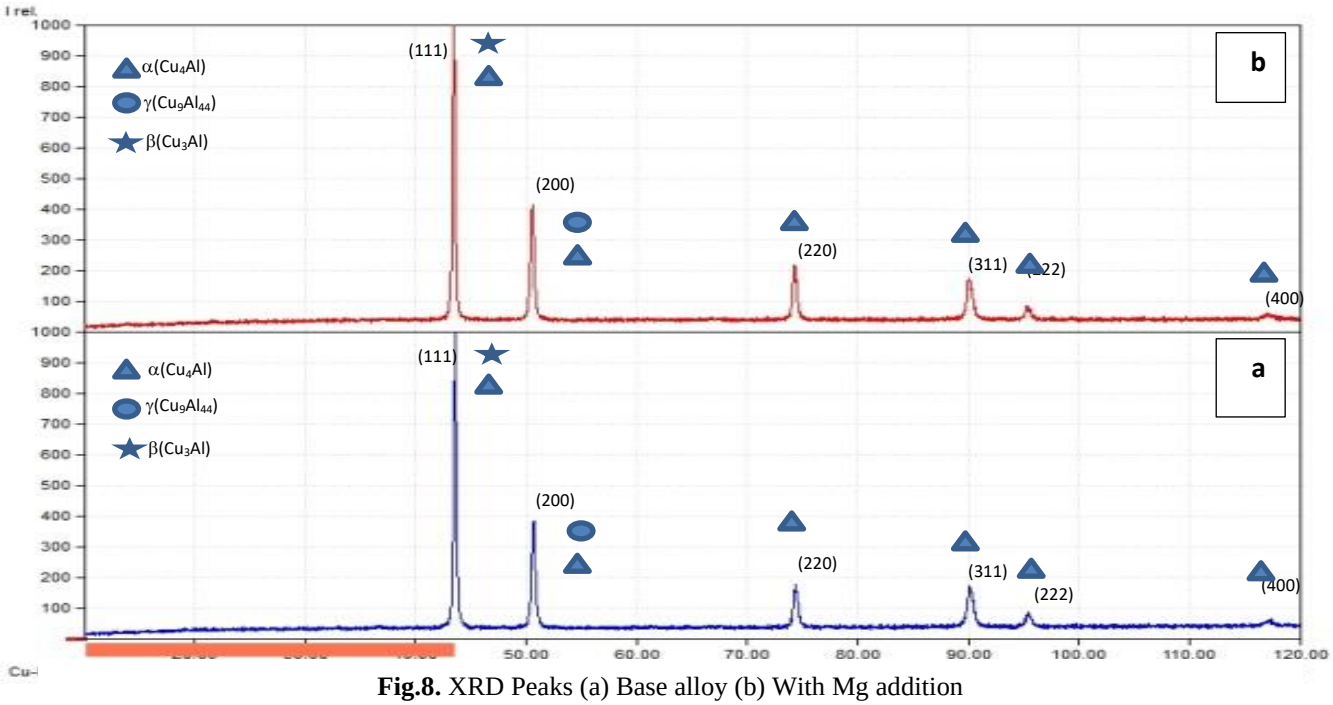

Fig.8. XRD Peaks (a) Base alloy (b) With Mg addition

Table 2.
X-Ray diffraction test results

Sp.	Peak No.	FWHM	Intensity
A	1	0.258	3393
	2	0.331	1288
	3	0.316	671
F	1	0.273	3104
	2	0.347	1146
	3	0.353	482

Fig.9. Optical Microscopy of the SMA

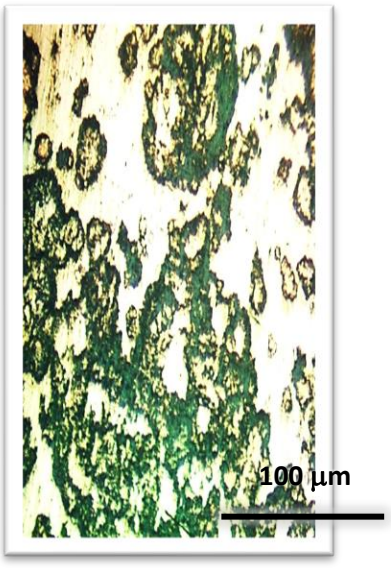

Fig.10. Optical Microscopy of the SMA alloy with (1.25%) Mg addition

5.2 Diametrical Compressive Strength

The effect of Magnesium volume fraction on the diametrical compressive strength is shown in Fig.11, the adding of Magnesium increases the diametrical compressive strength until it reaches the maximum value (24.26%) to the base alloy at Magnesium content (1.25%), this increase is due to the increase of hardness and density and decrease of porosity.

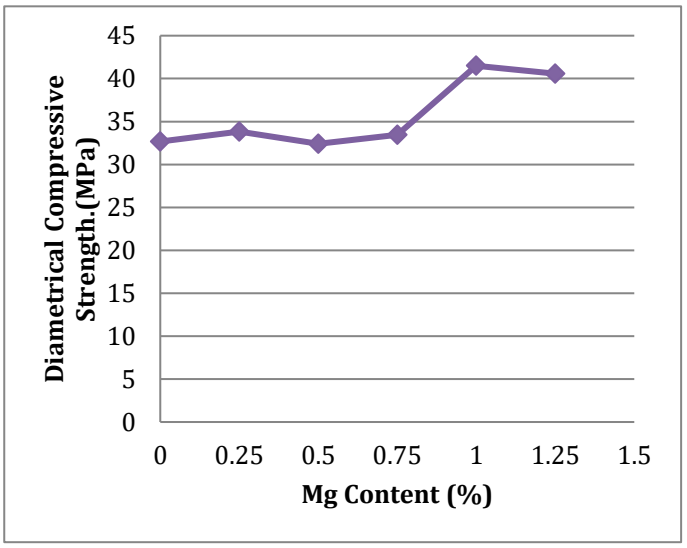

Fig.11. The Influence of Volumetric Fraction of Magnesium (Mg) On Diametrical Compressive Strength

3 Wear Rate

As we see in Fig.12 the wear rate decreases by increasing the volume fraction of Magnesium until it reaches the minimum value at magnesium content (1.25%) which decreases (83.10%) comparing to the base alloy and this decrease is due to the increase in hardness and density and decrease in porosity which enhance the cohesion between specimen particles and reduce the chance of separating them while sliding on the disc.

5.4 Differential Scanning Calorimetry (DSC)

The adding of magnesium to the (Cu-Al-Ni) alloy led to increase the austenite start temperature (As) and the austenite finish temperature (Af) with the ratio (0.08%) , (0.06%) respectively compared with the base alloy as shown in Figs. 13 and 14 and Table 3.

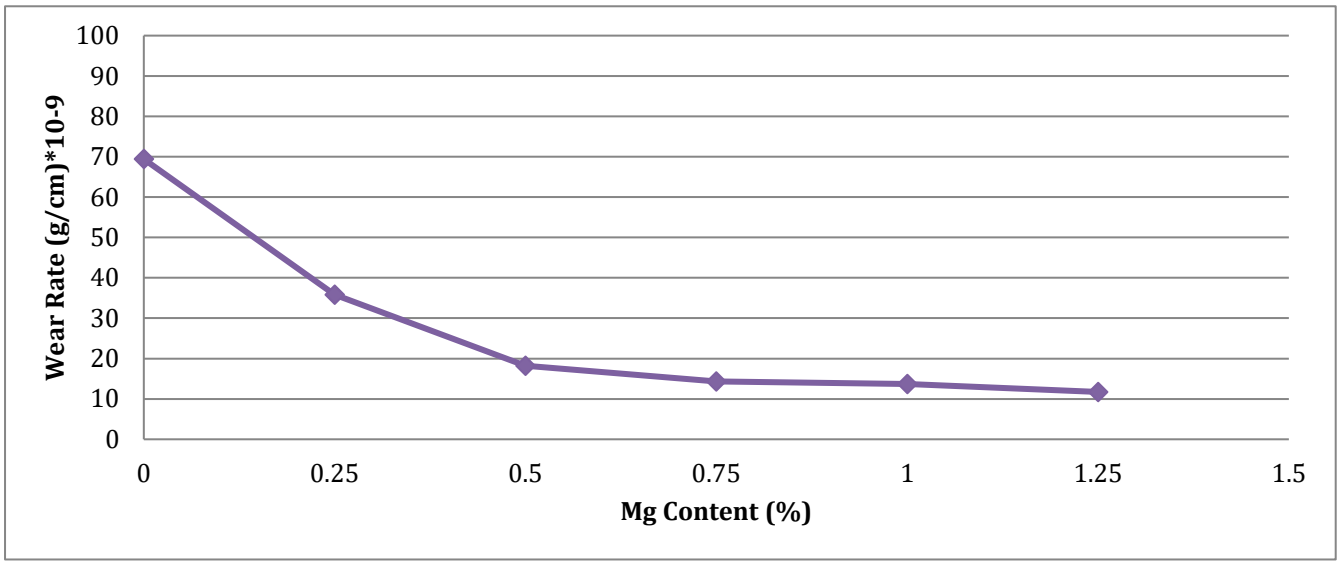

Fig.12. The Influence of Volumetric Fraction of Magnesium (Mg) On the wear rate

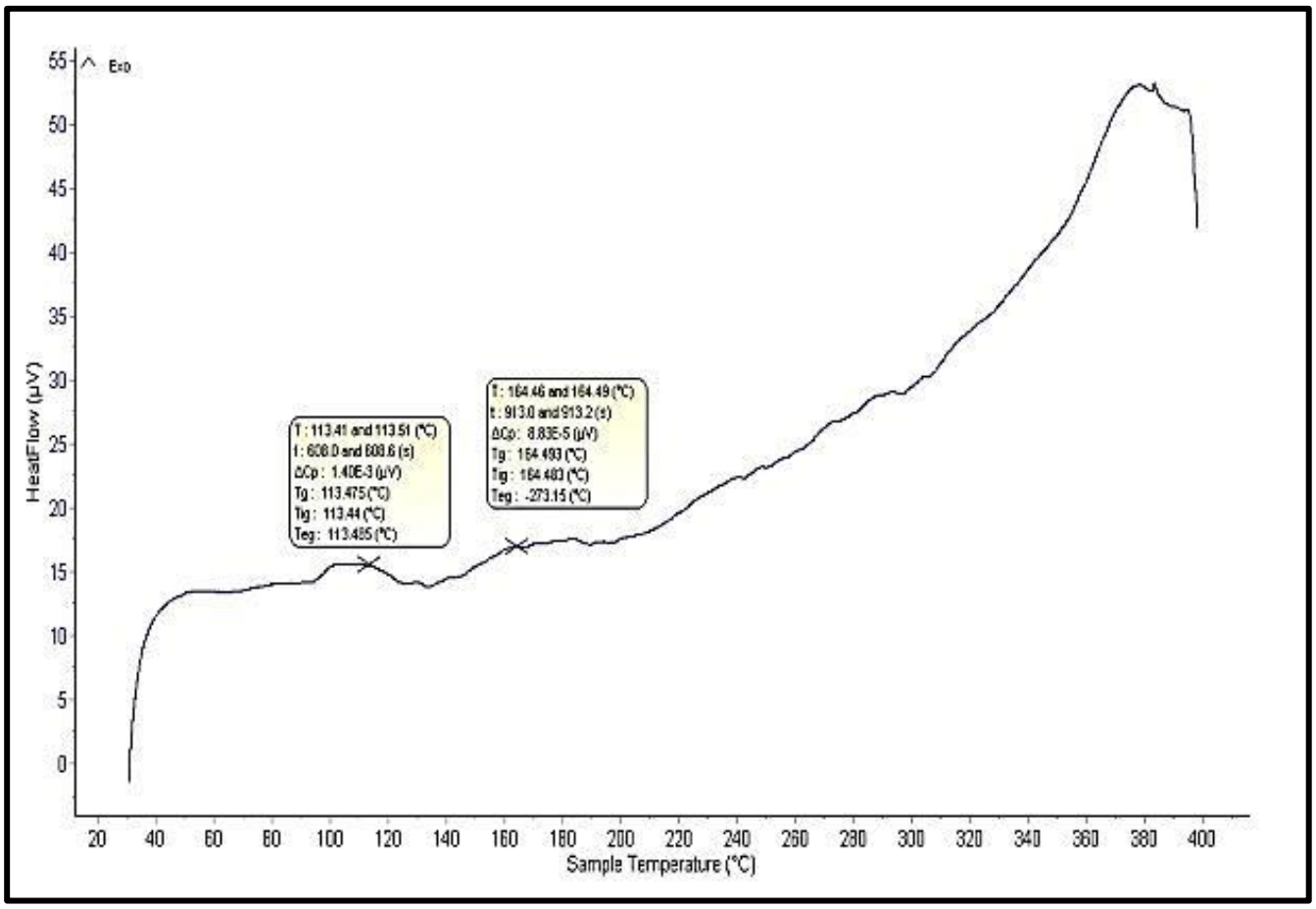

Fig.13. Differential Scanning Calorimetry of the (Cu-Al-Ni) alloy

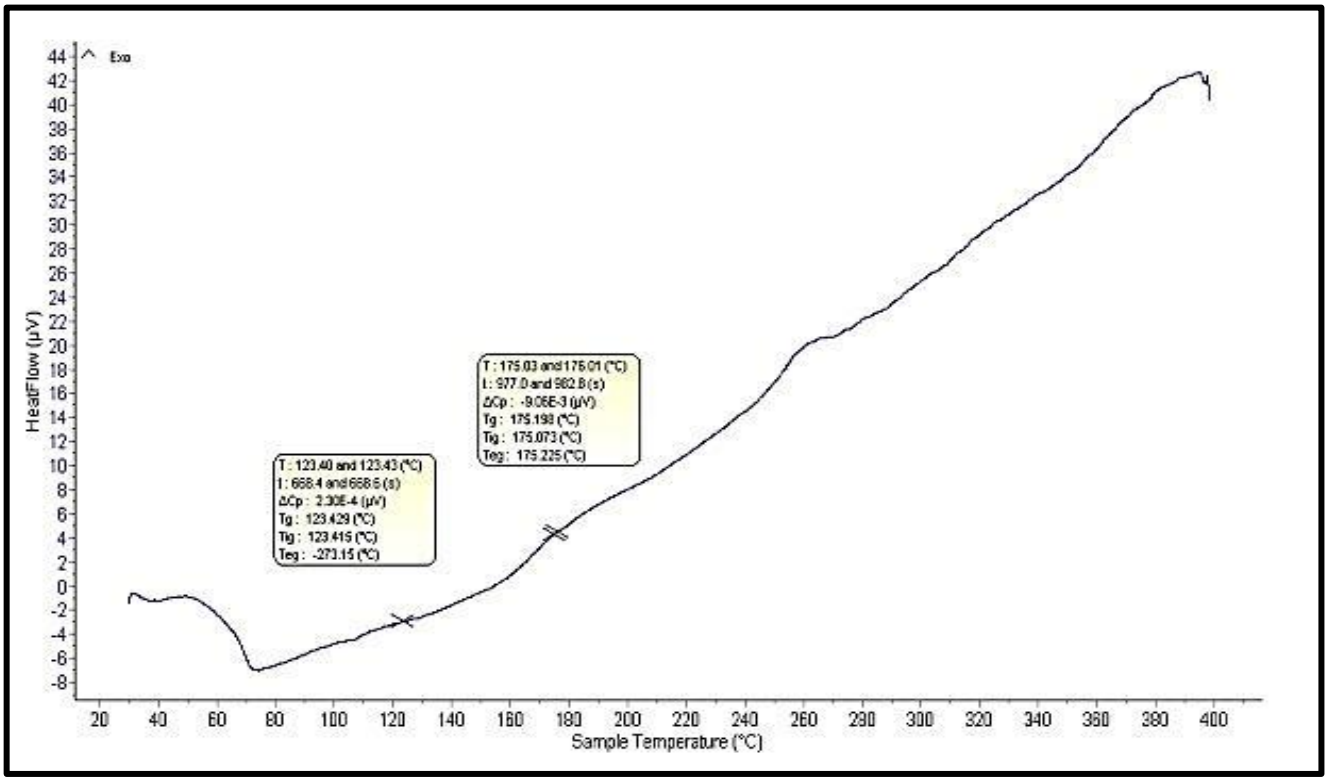

Fig.14. Differential Scanning Calorimetry of the (Cu-Al-Ni) alloy with (1.25%) Mg Content

Table 3
The transformation temperature from Martensite to Austenite

Spec.	Temp. (°C)	
	As	Af
A	113.5	164.5
F	123	175.5

3. Conclusion

1. The bulk density and the apparent density increase by increasing the volume fraction of Magnesium.
2. The apparent and the true porosity and the water absorption decrease by decreasing the volume fraction of Magnesium.
3. The hardness increases by adding Magnesium to the base alloy.
4. The diametrical compression stress increases by increasing the content of Magnesium.
5. The wear rate decreases by adding Magnesium to the (Cu-Al-Ni) alloy.
6. The (As) and (Af) temperature increases by adding Magnesium to the base alloy.

References

1. Rao, A., A.R. Srinivasa, and J.N. Reddy, *Design of shape memory alloy (SMA) actuators*. Vol. 3. 2015: Springer.
2. Lagoudas, D.C., *Shape memory alloys: modeling and engineering applications*. 2008: Springer.
3. Chang, L. and T. Read, *Plastic deformation and diffusionless phase changes in metals—The gold-cadmium beta phase.* JOM, 1951. **3**(1): p. 47-52.
4. Lecce, L., *Shape memory alloy engineering: for aerospace, structural and biomedical applications*. 2014: Elsevier.
5. Kim, J., et al., *Effects on microstructure and tensile properties of a zirconium addition to a Cu-Al-Ni shape memory alloy.* Metallurgical Transactions A, 1990. **21**(2): p. 741-744.
6. Saud, S.N., et al., *Influence of Silver nanoparticles addition on the phase transformation, mechanical properties and corrosion behaviour of Cu–Al–Ni shape memory alloys.* Journal of alloys and compounds, 2014. **612**: p. 471-478.

7. Saud, S.N., et al., *Effect of a fourth alloying element on the microstructure and mechanical properties of Cu–Al–Ni shape memory alloys.* Journal of Materials Research, 2015. **30**(14): p. 2258-2269.
8. Ali, A.R.K.A., *Study of Compression Behaviour of a Cu-13Al-4Ni-xCr Shape Memory Alloys Prepared by powder metallurgy process.* Journal of University of Babylon, 2017. **25**(1): p. 145-156.
9. Zhang, X., et al., *The enhancement of the mechanical properties and the shape memory effect for the Cu-13.0Al-4.0Ni alloy by boron addition*. Journal of Alloys and Compounds, 2019. **776**: p. 326-333.
10. Adnan, R.S.A., *Effect of Tin Addition on Shape Memory Effect and Mechanical Properties of Cu-Al-Ni Shape Memory Alloy*. Engineering and Technology Journal, 2020. **38**(8A): p. 1178-1186.
11. Razooqi, R.N., et al., *The Physical and Mechanical Properties of a Shape Memory Alloy Reinforced with Carbon Nanotubes (CNTs).* Tikrit Journal of Pure Science, 2018. **23**(9): p. 80-88.
12. Berger, M.B. *The importance and testing of density/porosity/permeability/pore size for refractories*. in *The Southern African Institute of Mining and Metallurgy Refractories Conference*. 2010.
13. Standard, A., *Standard test method for water absorption, bulk density, apparent porosity and apparent specific gravity for fired whiteware products.* Annual Book ASTM Standard, 2006. **15**: p. 112-3.
14. Lee, M., *X-Ray diffraction for materials research: from fundamentals to applications*. 2017: Apple Academic Press.
15. ALmohand, A., *preparing (Al-B4C) composite material and study some of their mechanical properties.* The Iraqi Journal for mechanical and material engineering, 2010. **10**(3).
16. Chawla, K.K., *Metal matrix composites.* Materials science and technology, 2006.